CHAPTER 6

FABRICATION AND CHARACTERIZATION OF ULTRAFAST ALL-OPTICAL SWITCH UTILIZING INTERSUBBAND TRANSITION

6.1 Growth and Characterization of GaN/AlN Multiple Quantum Wells on AlN

In this section, the growth of GaN/AlN MQW on the AlN buffer layer is described. It has been clearly shown in Chapter 5 that the MOVPE growth technique can give very high crystalline quality of AlN buffer layer, compared to that grown by MBE growth technique. However, in order to obtain the MQW structure that gives absorption at around 1.55 μm, optical communication wavelength, the growth of GaN/AlN MQW by MOVPE growth technique still has to deal with problems concerning interface roughness and thickness fluctuation, as the shortest wavelength of intersubband absorption in MOVPE-grown GaN/AlN MQW described in Chapter 3 was around 2 μm.

The growth of GaN/AlN MQW is therefore carried out by MBE growth technique in this study to eliminate such problems. However, since the MOVPE growth technique could give higher crystalline quality, the growth of AlN buffer layer on sapphire substrate is performed by MOVPE to achieve the best quality for the fabrication of optical waveguide.

After obtaining the high quality 1-μm-thick AlN buffer layers grown on sapphire substrate by the MOVPE growth technique, the growth of GaN/AlN MQW structures was then performed on the as-grown AlN buffer layer in the MBE growth chamber with the structure shown in Inset of Fig. 6.1. The number of MQW period was set to 40 periods, and the quantum wells were highly doped to obtain the carrier concentration of $1x10^{20}$ cm^{-3}, for the intersubband absorption measurements by Single-pass transmission method. During the growth, the growth temperature was set to be 800 °C, and the substrate was kept rotating to get good uniformity. Since the MQW is grown on AlN layer, the AlN barrier can be grown as thick as necessary without problems of cracking, etc. The AlN thickness is therefore set to be as thick as 10 nm, much thicker than those grown previously (3 nm). The AlN barriers are much thicker than the GaN quantum wells, resulting in the MQW layer with high Al composition. This could help reducing the lattice mismatch between AlN and MQW layer. The MQW can therefore be grown easily on the AlN layer without problems of cracking. This could therefore reduce the defects which could be generated by large lattice mismatch in the MQW structures, such as threading dislocations.

The characterization of the MQW was then performed by nomarsky microscope and XRD measurement. The surface morphology taken by nomarsky microscope revealed that the smooth surface morphology was obtained without any cracking observed. The cracking disappears when the material for buffer layer was changed from GaN to AlN, while the MQW layer was grown with the same amount of quantum wells, suggesting that the effect of lattice mismatch was reduced. This is therefore an evidence of improvement in strain-engineering in the MQW structure via the use of AlN buffer layer. Figure 6.1 shows the XRD $2\theta/\omega$ profile of 40-period GaN(1.4 nm)/AlN(11 nm) grown by MBE. As can be seen, the XRD profile shows satellite peaks with higher orders up to -9^{th} peaks, indicating that the MQW structure has very good structural quality with sharp interfaces, as a result of the MBE growth technique.

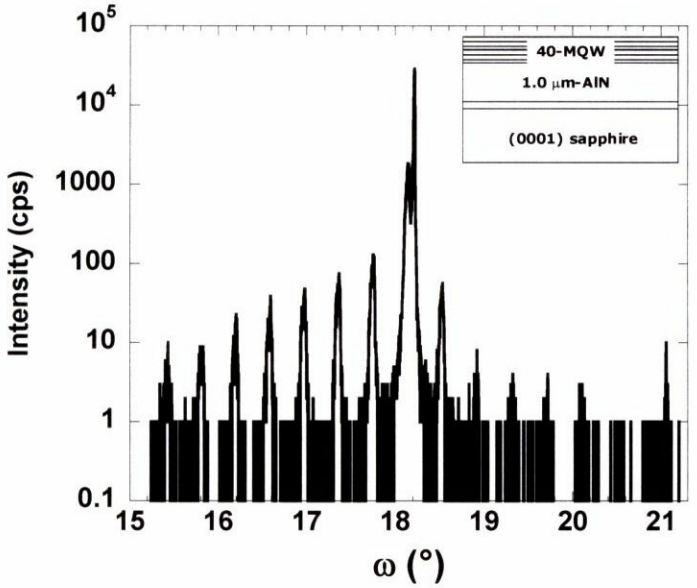

Figure 6.1 XRD ω/2θ scan profile of MBE-grown 40-period GaN/AlN MQW grown on MOVPE-grown 1-μm-thick AlN. Inset: Schematic structure.

In order to confirm the existence of intersubband absorption in the quantum wells grown on AlN layer, the intersubband absorption measurements were then performed by the Multiple-reflection method. Two samples which have different quantum well thickness, 2.0 nm and 2.5 nm, and the same barrier thickness (10.5 nm) were

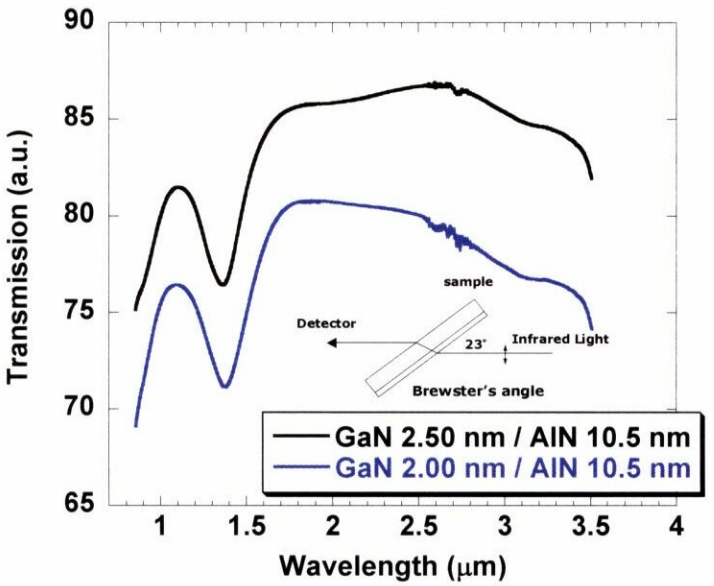

Figure 6.2 Transmission spectra of two GaN/AlN MQW with different quantum-well thickness measured by Multiple-reflection method

investigated. Figure 6.2 shows the transmission spectra of both samples taken for a 6-mm-long waveguide with 45° polished ends. The intersubband absorption was clearly observed at the wavelength of 1.35 μm for both samples, as seen in Fig. 6.2. It is therefore confirmed that the MBE-grown MQW structures grown on high quality AlN layer can achieve the intersubband absorption at wavelength shorter than 2 μm, including the optical telecommunication wavelength regime. It is also expected that an absorption wavelength at around 1.55 μm can be achieved with increasing the well thickness. This shows the possibility to achieve the intersubband absorption at both optical communication wavelengths (1.3 μm and 1.55 μm) with the MQW structures grown on AlN.

Considering the wavelength of intersubband absorption which shows no shifting even though the quantum well thickness was changed, the effect of built-in electric field is thought to be a main cause of such phenomenon. As described in Chapter 3, the built-in electric field induced by the lattice mismatch can bend the conduction band, causing a higher conduction band offset and resulting in blue-shifting of intersubband absorption wavelength. As the thin GaN quantum wells are grown on a thick AlN buffer layer, the stress induced by the lattice mismatch in the quantum well can be very large that it can generate very strong piezoelectric field. The induced built-in electric field is so strong that it can bend the conduction band to obtain the maximum conduction offset in the quantum well structure. Therefore, the wavelength of intersubband absorption is thought to be determined by the strength of the built-in electric field. This could be an advantage when the intersubband absorption wavelength can be set to a desired wavelength easily without shifting when the optimal quantum well thickness was found. Furthermore, since the built-in electric field is very strong in the structure, the realization of intersubband absorption at wavelength around 1.3 μm in the waveguide can be achieved with the AlN waveguide. This is also one of advantage over the GaN waveguide, where such wavelength could not be obtained as the built-in electric field is weakened when growing fewer number of quantum wells. However, since the intersubband absorption wavelength does not move when the well thickness change from 2.0 nm to 2.5 nm, tuning of the wavelength is another important issue that is necessary to be studied. The issue on the wavelength tuning is therefore discussed in Section 6.4.

6.2 Observation of Intersubband Absorption in AlN Waveguides with GaN/AlN Quantum Wells

In this section, the fabrication and characterization of AlN-based waveguide with GaN/AlN MQW structure is discussed. As the intersubband absorption in GaN/AlN MQW was successfully observed by the multiple reflection method as described in the last section, it is worth to study the characteristic of the AlN-based waveguide with GaN/AlN quantum wells. In this study, the waveguide structure as schematically illustrated in Fig. 6.3 was fabricated. Firstly, the 0.4-μm-thick AlN buffer layer was grown by low-pressure MOVPE technique. Then, the regrowth of two 2.0-nm-thick GaN quantum wells with 10.5-nm-thick AlN barriers were performed on the same wafer by MBE technique. Both of growth techniques were applied in order to obtain a good crystalline quality buffer layer and MQW layer that has absorption in the optical communication wavelength range. The quantum wells were doped with Si to obtain a carrier concentration of $1x10^{20}$ cm^{-3}. Consequently, the upper AlN cladding layer was also grown by MBE immediately after the growth of quantum wells have finished. It should be noted here that with such carrier concentration, only two quantum wells are enough to achieve the intersubband absorption of 20 dB in the waveguide structure. More number of quantum wells could provide too strong absorption which is not suitable for the device fabrication. However, the absorption from two quantum wells is supposed to be too weak for intersubband absorption measurements by the

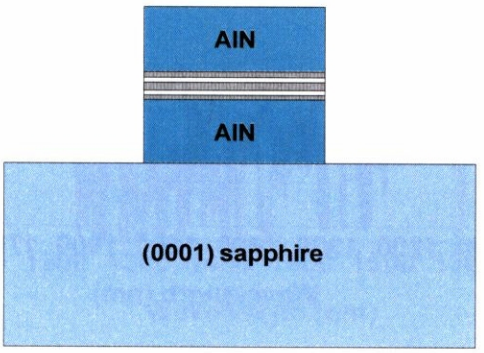

Figure 6.3 Schematic structure of AlN waveguide structure with GaN/AlN MQW

Multiple-reflection method. In this study, the measurement by the Multiple-reflection method was performed but, as expected, no absorption was observed in the sample. One might ask if the intersubband absorption from only two quantum wells is enough to be observed in the waveguide. The answer is "yes", because if one can couple the TM polarized light to waveguide, the absorption in the TM mode is supposed to be very strong, especially for the quantum wells doped with carrier concentration over $1x10^{19}$ cm^{-3}, with the measurements by the Waveguide coupling method.

In order to measure the intersubband transition by Waveguide coupling method, the waveguide was fabricated. The wafer surface was firstly coated by SiO_2 by sputtering method. Then the waveguide patterns were formed by photolithography and then etched by ICP etching technique to fabricate the high-mesa waveguide. The waveguide characterization was then performed by the waveguide coupling method using the supercontinuum light source. Figure 6.4 shows the transmission spectra of a 400-μm-long as-fabricated waveguide for TM and TE polarization measured by Waveguide-coupling method. The difference between TM and TE polarization (TM-TE), showing the intersubband absorption spectrum in log scale, was then calculated as shown in Fig. 6.5. Obviously it can be seen in Fig. 6.5 that the intersubband absorption

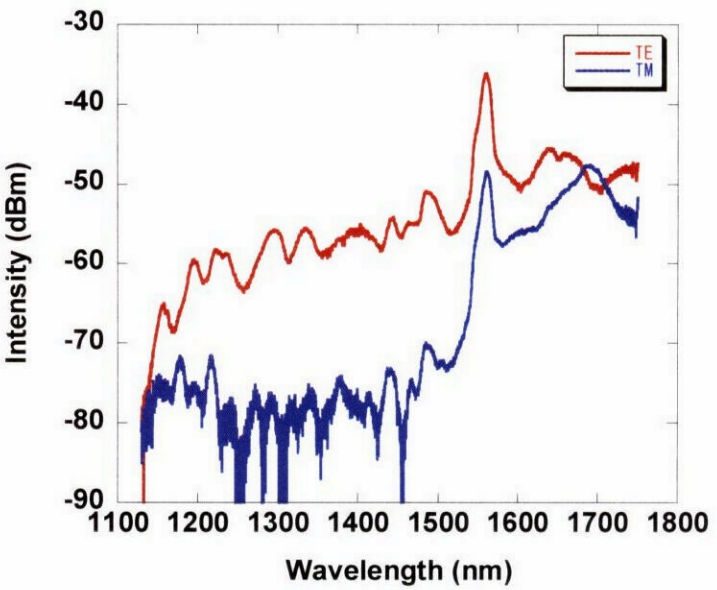

Figure 6.4 TM and TE mode transmission spectra of as-fabricated AlN high mesa waveguide with two GaN/AlN quantum-wells measured by Waveguide-coupling method using supercontinuum light source

exists in the waveguide with the absorption peak at 1.35 μm. The difference between TM and TE mode is found to be almost zero at the short wavelength around 1.1 μm, and at the long wavelength around 1.7 μm. This clearly shows that there is no additional TM polarization loss that is caused by crystalline defects inside the waveguide, suggesting that the waveguide structure was fabricated with high crystalline quality. The absorption peak at 1.35 μm shown in Fig. 6.5 is at the same wavelength as that of intersubband absorption in Fig. 6.2, and is the shortest wavelength ever observed in the waveguide structure. The unchange of wavelength could be explained by an effect of very strong built-in electric field induced in the quantum wells grown on AlN buffer layer, as described in the last section. This built-in electric field is very strong because only GaN quantum wells are strained inside the AlN waveguide. The effective conduction band offset in the structure is supposed to be bent by the built-in electric field to be at maximum even for a single quantum well. Therefore there is no big change in built-in electric field either the MQW structure contains 2 or 40 quantum wells.

It should be reminded here that for MQW grown on GaN, the thickness of AlN barrier cannot be grown thicker than 3 nm owing to the critical thickness of AlN on GaN. Growing of AlN on GaN layer with a thickness of over 3 nm could therefore

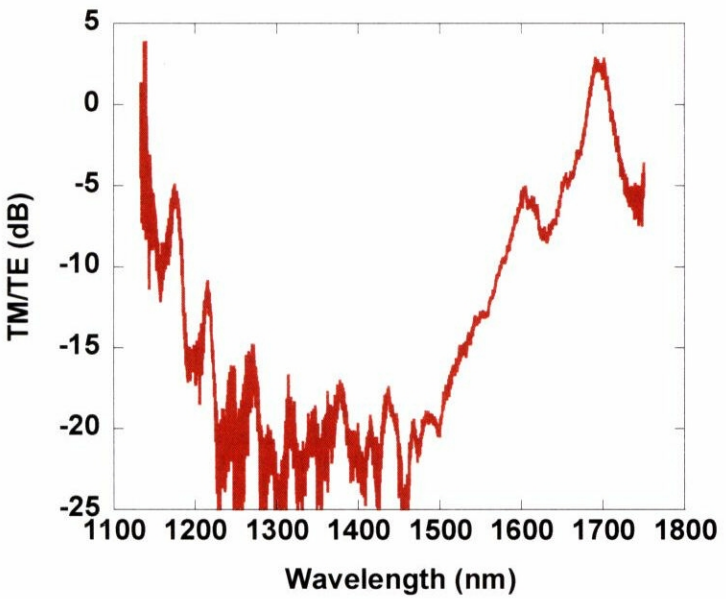

Figure 6.5 Intersubband absorption spectrum of as-fabricated AlN high mesa waveguide with two GaN/AlN quantum-wells measured by Waveguide-coupling method using supercontinuum light source

result in bad crystalline quality and cause cracking problems. In case of the MQW grown on GaN layer, the stress induced in the MQW layer changes with the total thickness of MQW layer. This thus induces a change in the strained induced built-in electric field. The built-in electric field is therefore strongly dependent on the number of quantum wells and the total thickness of MQW layer to be grown. Note that the larger built-in electric field, the larger blue shifting of intersubband absorption wavelength. (See Appendix D) This is why 40-period-MQW on GaN layer always gives shorter intersubband absorption wavelength than 2-period-QW on GaN layer, as described in Chapter 4. In GaN waveguide, this could be a problem in tuning absorption wavelength of a waveguide since the absorption in only two-period quantum wells cannot be detected by the Multiple reflection method, so 40 periods MQW sample is normally used. However, because of the different built-in electric field in 2-period-QW and 40-period-MQW samples, the wavelength shifting causes many difficulties in tuning the wavelength. In this study, the growth of MQW on AlN layer has shown that such problem does not exist. With thick AlN barriers, the GaN quantum well is highly strained inside the structure, and the internal electric field is considered to be at the maximum for each quantum well. An increase in the numbers of quantum wells therefore does not affect much to the strength of built-in electric field in this case, thus not inducing any shifting of intersubband transition wavelength with different numbers of quantum wells. This is very convenient for the fabrication of optical devices, because the wavelength of intersubband transition can be firstly tuned by growing 40-period MQW which can be measured by the Single-pass transmission method. Then after achieving the desired wavelength, the final growth can be done by growing the same structure, but just reducing the number of quantum wells, and growing the upper cladding layer for the waveguide fabrication. These processes can be performed to achieve the same intersubband absorption wavelength without any concerns of unintentionally wavelength shifting. It is therefore another advantage of the AlN waveguide over the GaN waveguide. Furthermore, in case of MQW grown on AlN, if the thickness of GaN quantum well is thinner than the critical thickness, the thickness of AlN barrier can be grown as thick as desired. This is because as long as the GaN is thin enough, the lattice relaxation does not occur, so the growth of AlN barrier in this case is not different with the growth of thick bulk AlN. Moreover, if one considers the MQW

layer as AlGaN layer, the Al composition in such AlGaN layer raises with increasing AlN barrier thickness. The lattice constant of AlGaN layer therefore gets close to that of AlN layer with thick barrier, making it easy to grow the structure in the view point of strain engineering in the crystal growth. With these results, it can therefore be concluded that the AlN waveguide with GaN/AlN MQW is a promising structure for the realization of intersubband transition devices.

6.3 Intersubband Absorption Saturation in AlN Waveguide with GaN/AlN Quantum Wells

One of the important characteristics of the intersubband absorption is its "*saturable absorption*". It is the principle of the ultrafast all-optical switching utilizing intersubband transition. The intersubband absorption in a waveguide can be saturated by exciting carriers in the first subband energy level of the quantum wells to the second subband energy level. This can be achieved by pumping the waveguide with ultrashort optical-pulse at high energy. In this section, the demonstration of the intersubband absorption saturation in AlN waveguide with GaN/AlN quantum wells is described.

6.3.1 Experimental setup

The absorption saturations and switching performances of the waveguide were characterized by a measurement system schematically shown in Fig. 6.6. In order to demonstrate the saturation of intersubband absorption, ultrashort optical pulse with high pulse energy is necessary. The optical pulses used in this study were therefore generated by an optical parametric oscillator (OPO) excited by a mode-locked Ti:sapphire laser with a repetition rate of 80 MHz. With this optical pulse generation, the signal pulses with a wavelength of 1.55 μm and idler pulses with a wavelength of 1.7 μm can be generated as signal and control pulses, respectively, for the switching experiments. The pulse widths of the OPO outputs for both signal and control pulses are nominally 130 fs, which is applicable for the ultrafast switching experiments.

The polarization of both signal and control pulses were controlled by wave plates. Pulse intensities were controlled by ND filters, wave plates and polarizers, before

coupling to the optical fiber through a collimating lens. The optical fiber used in this study was a polarization-maintaining dispersion-shifted fiber. The total length of the fibers throughout the light path was set to be as short as 1.0 metre in order to reduce the dispersion effect which can broaden the pulse widths. As a result, it have been confirmed that the pulse width was unchanged for the 1.55-μm optical pulses propagating through the polarization-maintaining dispersion-shifted fiber. However, the pulse width is considered to be broadened to some extent for the 1.7-μm optical pulses due to dispersion in the fiber. At the end of the optical path, output signals were detected by an InGaAs detector, whereas control pulses were cut by a band-pass filter in front of the detector as shown in Fig. 6.6 (c).

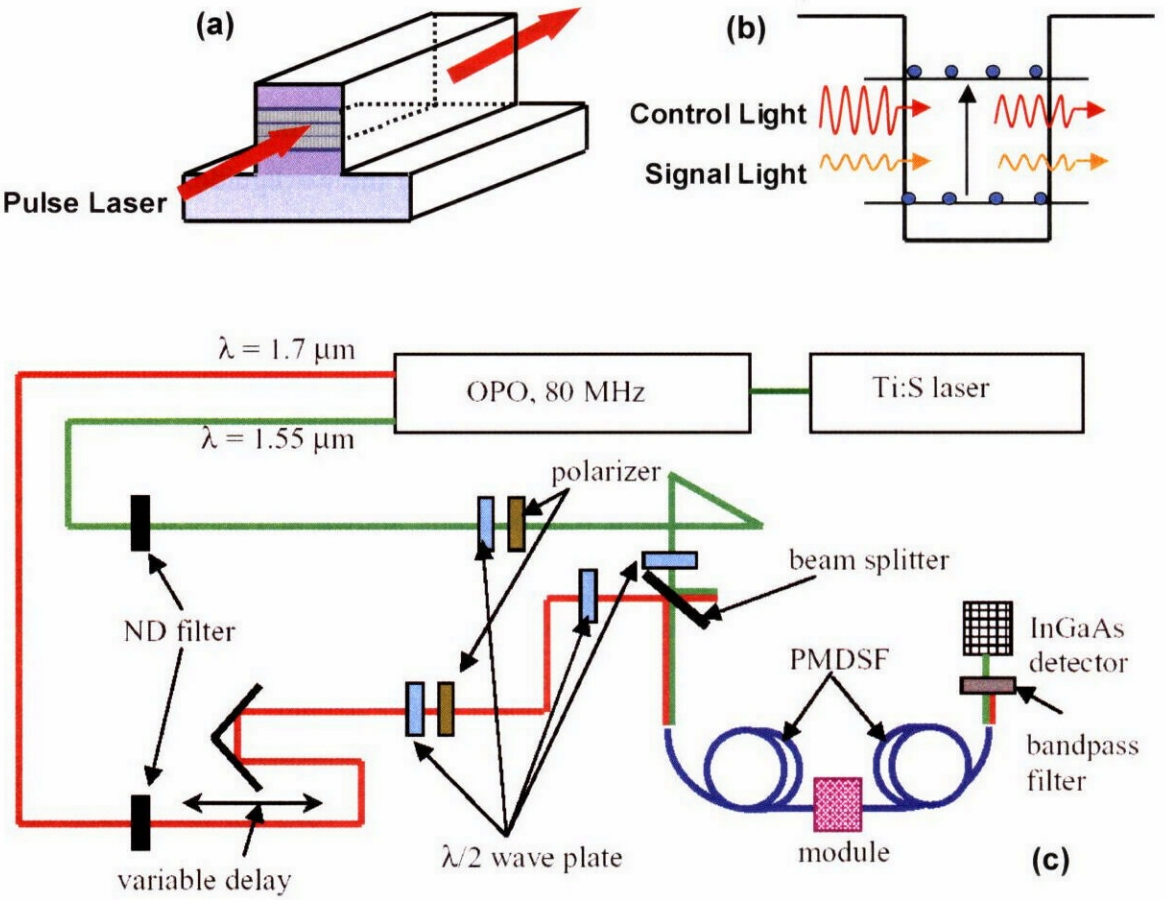

Figure 6.6 (a) Schematic diagram of a waveguide with pumping pulse laser
(b) Schematic diagram of MQW at absorption-saturated state
(c) Measurement setup for absorption saturation observation [62]

6.3.2 Demonstration of intersubband absorption saturation

Before moving to the demonstration of intersubband absorption saturation, an important parameter in this experiment, *insertion loss*, is described here. The insertion loss of a waveguide usually means optical loss occurred throughout the light path from one side of the waveguide to the other side, including the fiber coupling part. It therefore means a combination of fiber-to-waveguide coupling loss and the waveguide propagation loss, generally measured by finding a difference of the optical power between input fiber and output fiber. For TE-polarization, the insertion loss is dominated by the fiber-to-waveguide coupling loss, while the propagation loss is also included but much less than the coupling loss. This is because the waveguide used in the measurement is usually not longer than 1 mm; considering the 10 dB/cm loss of AlN waveguide estimated in Chapter 5, the propagation loss should be only 1 dB for 1-mm-long waveguide. The fiber-to-waveguide coupling loss, on the other hand, is around 10 dB in this experiment for the coupling with taper fiber. The TE-polarization loss can therefore be used as an indicator of waveguide coupling condition. For TM-polarization, besides the coupling loss and intrinsic propagation loss, extra propagation loss is induced by the intersubband absorption. In addition, the extra propagation loss can be also induced by the threading dislocations and other crystalline defects existing in the waveguide. In other words, the difference of insertion loss between TM-polarization and TE-polarization can be estimated as a summation of the intersubband absorption loss and the propagation loss generated by crystalline defects. The insertion losses of both TM-polarization and TE-polarization are thus very important parameter that is needed to monitor for the observation of intersubband absorption saturation.

The intersubband absorption saturation of the GaN/AlN MQW on AlN-based waveguide structure was therefore studied by monitoring the change of insertion loss of TM-polarization and TE-polarization using optical pulses generated by the OPO system as input light. A high-mesa AlN waveguide, of which its intersubband absorption spectrum was taken by the waveguide coupling method as already shown in Fig. 4.13, was used in this study. As can be seen in Fig. 6.5, the peak wavelength of the intersubband absorption is at around 1350 nm with TM/TE distinction ratio of around 25 dB. However, since the OPO system used in this study cannot generate the optical pulses at a wavelength of 1350 nm, the intersubband absorption saturation has been

studied at other two wavelengths, 1425 nm and 1494 nm, instead.

The wavelength of 1425 nm is the shortest wavelength that can be tuned by the OPO system used in this study. The spectrum of output optical pulse from OPO system at this wavelength is shown in Fig. 6.7. In general this wavelength is interfered by the water vapor absorption which always exists in the air. The spectrum of the output pulse is therefore distorted as seen in Fig. 6.7. Even though the distortion and noise in the optical pulse, the intersubband absorption saturation was clearly observed as shown in

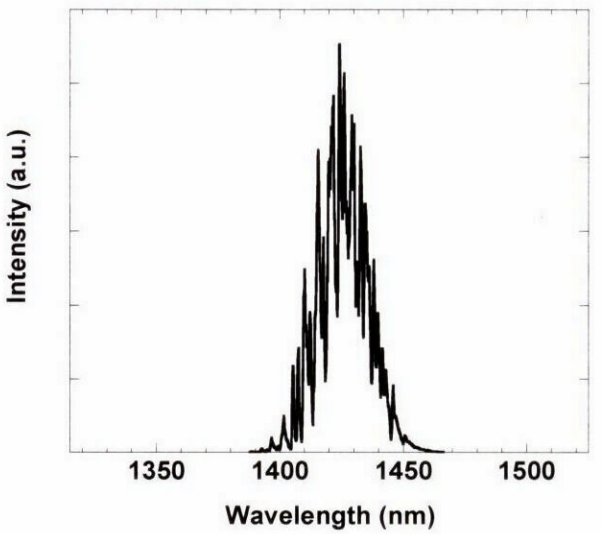

Figure 6.7 Spectrum of input optical pulse at 1425 nm generated by OPO system

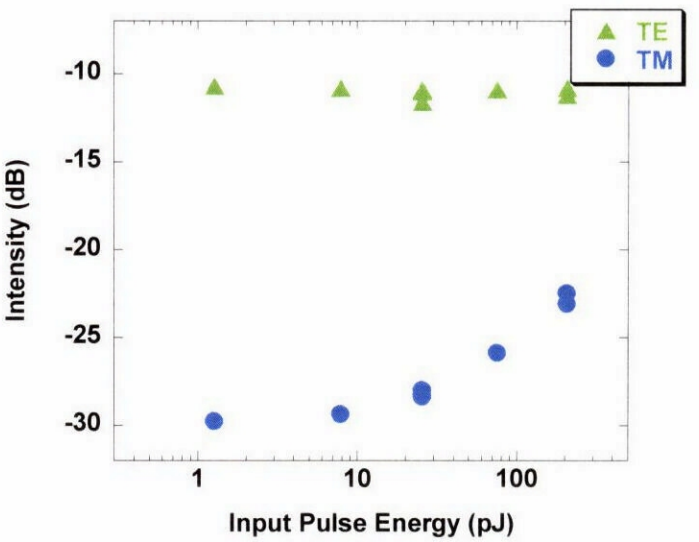

Figure 6.8 Fiber-to-fiber insertion loss of TM and TE polarization as a function of input pulse energy

Fig. 6.8. For TE-polarization, the insertion loss is approximately 11 dB, almost unchanged with increasing input pulse energy from 1 pJ to 200 pJ. On the other hand, the insertion loss of TM-polarization decreases with increasing input pulse energy; the insertion loss changed from -30 dB to -23 dB when the input pulse energy increased from 1 pJ to 200 pJ. This result obviously shows that the intersubband absorption saturation by 7 dB was achieved with the input pulse energy of 200 pJ. Although more absorption saturation is expected for higher input pulse energy, it cannot be observed in this experiment because the pulse energy is limited by the maximum output power of the OPO system. With this experimental result, however, the intersubband absorption saturation has been observed in the AlN waveguide with the shortest wavelength ever reported, 1425 nm.

In order to avoid the effect of distortion and noise from the water vapor absorption, the observation of intersubband absorption saturation was also performed for the optical pulse at wavelength of 1494 nm. This optical pulse has a clear spectrum without noise from water vapor absorption as shown in Fig. 6.9. However, the insertion loss decreases to -21 dB at this wavelength, 9 dB less than insertion loss at 1425 nm, which is considered to be a result of decreasing intersubband absorption only. The intersubband absorption saturation at 1494 nm is observed as shown in Fig. 6.10. The insertion loss

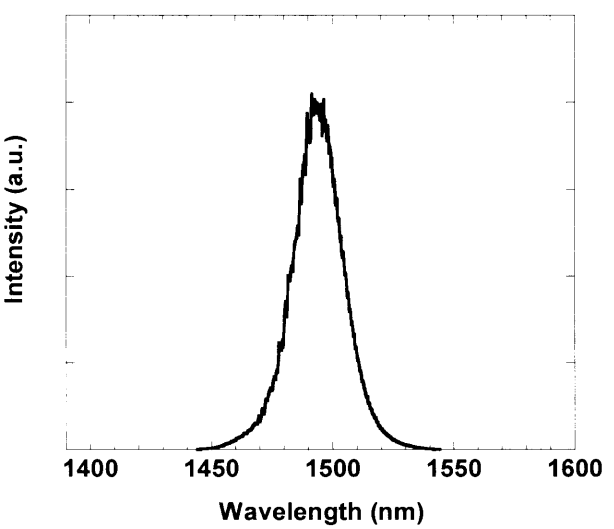

Figure 6.9 Spectrum of input optical pulse at 1494 nm generated by OPO system

was unchanged with increasing input pulse energy for TE-polarization, whereas the intersubband absorption saturation by 3.5 dB was observed for TM-polarization with input pulse energy of 120 pJ. This reduced absorption saturation is considered to be caused by a decrease in intersubband absorption distinction ratio at 1494 nm. More absorption saturation is therefore expected with input optical pulse at shorter wavelength, especially at the absorption peak wavelength of 1350 nm. At the wavelength of 1350 nm, larger distinction ratio from intersubband absorption could be obtained, and the spectrum of input optical pulse should be clear with no noise from water vapor absorption; thus it is expected that the absorption saturation could be achieved with low input pulse energy. It is therefore believed that this device can be used for the ultrafast all-optical switching at the optical communication wavelength of 1.3 μm, which is the shortest operating wavelength ever reported for the intersubband transition devices. Such operating wavelength therefore shows possibility in using the device for ultrafast all-optical processing with dual wavelengths of both 1.3 μm and 1.55 μm, covering two main optical-communication wavelength regimes.

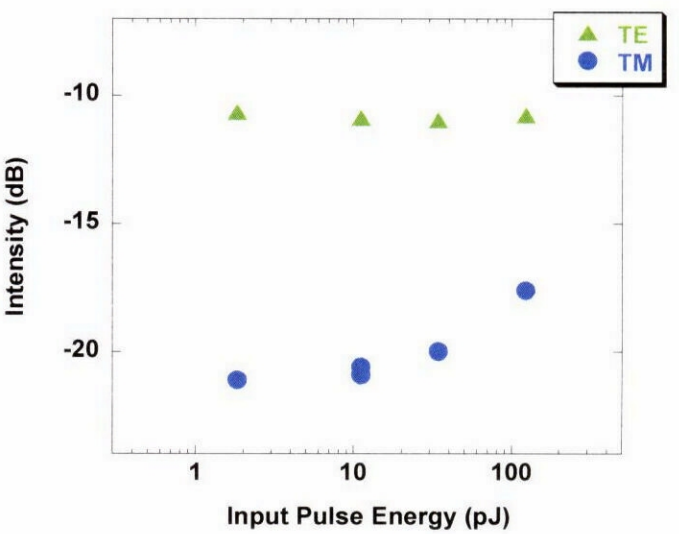

Figure 6.10 Fiber-to-fiber insertion loss of TM and TE polarization as a function of input pulse energy